**Online Date Supplement**

# Role of glucosylceramide in lung endothelial cell fate and emphysema

Kengo Koike, Evgeny V. Berdyshev, Andrew M. Mikosz, Irina A. Bronova, Anna S. Bronoff, John P. Jung, Erica L. Beatman, Kevin Ni, Danting Cao, April K. Scruggs, Karina A. Serban, and Irina Petrache

## Supplemental method

*Reagents*

Genz-123346 (Genz) was purchased from Medchem Express LLC (Monmouth Junction, NJ). N-(1-Adamantaneacetyl)-glucosylceramide (admantyl GlcCer) was obtained from Matreya LLC (State College, PA). Bafilomycin A1 was purchased from LC laboratories (Woburn, MA). MES, Nigericin, Methanol, water, and chloroform (LC/MS or HPLC grade) were obtained from Thermo Fisher Scientific (Waltham, MA).

*Development and evaluation of chronic CS-induced or elastase-induced pulmonary emphysema in mice*

C57BL/6 mice (two months old, four females and males) were exposed to

cigarette smoke (CS) or ambient air control (AC) for 6 months (E1). Briefly, mice were exposed for 4 hours to 11% mainstream and 89% side-stream smoke from reference cigarettes (Tobacco Research Institute, Lexington, KY), using a Teague 10E device apparatus (Teague Enterprises, Davis, CA). Control mice underwent the same sleep cycle disruption and stimulation via transportation. Research reference cigarettes (3R4F) were purchased from the Tobacco Research Institute (University of Kentucky, Lexington, KY). BALB/c mice (two months old, male, *n* = 8-12/group) were anesthetized with isoflurane, and either 1.5 U, 3 U, or 6 U/mouse of porcine pancreatic elastase (EC134, Elastin Products Company, Owensville, MO) dissolved in 60 μl of physiological saline solution was instilled via the trachea (E2). Control mice received saline alone. Either after 6 months of CS-exposure or 28 days after elastase administration, mice lungs were processed following euthanasia (E3). Morphometric analysis was performed on coded slides using a macro developed by R.M Tuder for MetaMorph (E4).

*Transfection of primary human lung microvascular endothelial cells*

Knockdown – Non targeting siRNA control (siNT, D-001206-14-05) and GCS

siRNA (siGCS, L-006441-00-0005) were obtained from Dharmacon (Lafayette, CO). Transfection was performed with Lipofectamine RNAiMAX reagent (13778150, Invitrogen, Carlsbad, CA) according to the manufacturer's specifications. Primary human lung microvascular endothelial cells (HLMVECs) were transfected with 5 nM of each siRNA for 24 or 72 hours.

Overexpression - GCS expression vector (RG206288) and empty control vector (PS100010) (pCMV6-Entry, mammalian vector with C-terminal turbo GFP tag) were purchased from OriGene Technologies Inc. (Rockville, MD). Transfection was performed with Lipofectamine™ LTX with PLUS™ reagent (15338100, Invitrogen) according to the manufacturer's specifications. HLMVECs were transfected with 1 μg of each plasmid for 24 hours.

*Western Blot*

Following treatments, culture media was washed on ice with phosphate buffered saline (PBS) and gently scraped with PBS. Cells were then spun at 16,000 g for 10 minutes at 4 °C, the supernatant was discarded, and the pellets were snap frozen at –80°C until use. For immunoblot analysis, either cell pellets or lung

tissues were thawed at 4°C in RIPA buffer (R0278, MilliporeSigma) containing a phosphatase inhibitor (04906837001, Roche Diagnostics, Indianapolis, IN) and protease inhibitor (04693116001, Roche Diagnostics) then sonicated and vortexed. After the cell lysate were centrifuged at 16,000 g for 10 minutes at 4 °C, the supernatant was used for assays. Protein concentration was determined by a bicinchoninic assay (BCA) (Pierce Biotechnology, Inc., Rockford, IL) using bovine serum albumin as a standard. Western blots were performed as described previously (E5). Briefly, equal amounts of protein (10-50 µg) were resolved by SDS-PAGE and transferred onto a polyvinylidene difluoride membrane (EMD Millipore). Membranes were blocked with either 5% nonfat milk in Tris-buffered saline, 0.1% Tween 20 (TBS-T) or Protein-Free T20 blocking buffer (Thermo Fisher Scientific Inc.) and incubated with diluted primary antibodies at 4°C overnight per manufacturers' specifications. Membranes were probed with the following primary antibodies: anti-vinculin (1:10,000, ab18058, Abcam, Cambridge, MA), anti-β-actin (1:6000, A5441, MilliporeSigma), anti-GAPDH (1:3000, ab9485, Abcam), anti-LC3B (1:50,000, L7543, MilliporeSigma), anti-SQSTM1/p62 (1:10,000, H00008878-M01, Abnova, Taipei, Taiwan), anti-phospho-mTOR (Ser2448) [1:500, 5536, Cell Signaling

Technology (CST), Danvers, MA], anti-mTOR (1:500, 2983, CST), anti-phospho-p70S6K (Thr389) (1:500, 9205, CST), anti-p70S6K (1:500, 9202, CST), anti-phosho-S6 Ribosomal Protein (1:4000, Ser235/236) (2211, CST), anti-S6 Ribosomal Protein (1:4000, 2217, CST), anti-phospho-AKT (Ser473) (1:1000, 4060, CST), anti-AKT (1:1000, 9272, CST), anti-phospho-AMPK$\alpha$ (Thr172) (1:1000, 2535, CST), anti-AMPK$\alpha$ (1:1000, 2532, CST), anti-phospho-eIF2a (Ser51) (1:500, 3597, CST), anti-eIF2$\alpha$ (1:500, 9722, CST), anti-Bax (1:1000, 2772, CST), anti-Bcl-2 (1:1000, ab196495, Abcam), anti-PARP1 (cleaved p25) (1:1000, ab32064, Abcam), anti-cleaved caspase-3 antibody (1:500, ab13847, Abcam), anti-turbo GFP antibody (1:4000, PA5-22688, Thermo Fisher Scientific), and anti-glucosylceramide synthase (GCS) antibody (1:1000, ab124296, Abcam). HRP-conjugated secondary antibodies (goat anti-rabbit/mouse, HRP conjugate) (45001175/45001187, GE Healthcare Life Sciences, Logan, UT) were used and blots were exposed to Luminata Forte (WBLUF0500, EMD Millipore) for chemiluminescent reaction. Images were taken with a ChemiDoc XRS system with Image Lab software (Bio-Rad). Densitometric analysis was performed with ImageJ 1.49 software (National Institutes of Health, Washington, DC).

*Immunofluorescence microscopy*

Cells were cultured on Nunc Lab-Tek II chamber slides (154526, Thermo Fisher Scientific) and treated as indicated. To stain autophagosomes and lysosomes, cells were incubated with DAPGreen (50 nM) (D676-10, Dojindo Molecular Technologies) and LysoTracker deep red (25 nM) (L12492, Thermo Fisher Scientific) in the culture medium for 30 minutes at 37°C (E6). Cells were washed with PBS and fixed with 4% paraformaldehyde for 30 minutes at room temperature followed by a second wash with PBS. After fixation, slides were mounted using ProLong Gold with DAPI (P36931, Thermo Fisher Scientific). Fluorescence imaging was preformed using a Zeiss LSM 700 confocal microscope using Zen Black v14 software. Images were acquired as 12-bit file format with both Zeiss 20x/0.8 M27 Plan-Apochromat and Zeiss Plan-Apochromat 63x/1.40 oil DIC M27 objectives. Post imaging processing was performed using ImageJ v2. Z-stacks were rendered using “max intensity” and the gamma was adjusted to reduce the background.

*Messenger RNA (mRNA) studies*

Total ribonucleic acid (RNA) was extracted from cultured cells using RNeasy Mini kit (Qiagen, Germantown, MD). 1000 ng of total extracted RNA was used to synthesize complementary DNA (cDNA) by High-Capacity cDNA Reverse Transcription kit (Applied Biosystems Inc., Foster City, CA). Real-time quantitative real-time polymerase chain reaction (qPCR) was performed on the StepOnePlus System using Taqman Universal PCR Master Mix (Applied Biosystems Inc.) and Taqman probe: UDP-glucose ceramide glucosyltransferase (Hs00234293_m1, Thermo Fisher Scientific). Relative mRNA expression was calculated using the double delta Ct method and 18s RNA endogenous control (Hs99999901_s1, Thermo Fisher Scientific).

*Sphingolipids determination*

Standards and reagents - Most lipid standards were purchased from Avanti Polar Lipids (Alabaster, AL) with the exception of some glycolipids which were purchased from Matreya, Inc (State College, PA). The standards were dissolved in methanol and stored at -20°C. UDP-α-D-Glucose was obtained from EMD Millipore (Burlington, MA).

Lipid extraction and sample preparation for LC-MS/MS – Lipids from plasma (0.05 ml), BAL (up to 0.5 ml) or cells were extracted by modified Bligh and Dyer procedure (E7) with the use of 2% formic acid for phase separation. Internal standards (D7-ceramide (N-palmitoyl-D-erythro-sphingosine (d7), 12:0-sphingomyelin (N-(dodecanoyl)-¬sphing-4-enine-1-phosphocholine), (d7)-sphingosine, (d7)-sphingosine-1-phosphate, and N-omega-CD3-Hexadecanoyl-glucopsychosine) were added at the beginning of the extraction process. Total lipid phosphorus content in the samples was determined using a phosphomolibdate reagent as dewscribed in (E8).

UHPLC-ESI-MS/MS analysis of glycosylceramides, ceramides, sphingoid bases, sphingosine-1-phosphate, and sphingomelins – The content of all sphingolipids was determined by liquid chromatography electrospray ionization tandem mass spectrometry using Sciex 6500QTRAP mass spectrometer coupled with Shimadzu Nexera X2 UHPLC system in scheduled multiple reaction monitoring (MRM) mode. Chromatography was performed using Ascentis Express RP-Amide 2.7 μm 2.1 x 50 mm column and gradient elution from methanol:water:formic acid (65:35:0.5) to methanol:chloroform:water:formic

acid (90:10:0.5:0.5) with both systems having 5 mM ammonium formate. All ceramides were detected in positive ions mode by monitoring transitions from corresponding molecular ions to the m/z 264.2 while dihydroceramides were detected by monitoring transitions to the m/z 284.2. Sphingomyelins were detected as a transition from molecular ions to the m/z 184.1. Sphingoid bases were detected through the loss of water from corresponding molecular ions. Glucosylceramides were detected as a transition from corresponding molecular ions to the m/z 264.2 (glycosylceramides) or to the m/z 284.2 (dihydroglycosylceramides). Sphingosine-1-phosphate and dihydrosphingosine-1-phosphate were detected in negative ions mode after acetylation as described in (E9). For lipid quantitation, standard curves of variable amounts of analytes versus fixed amount of the internal standards were created using available lipid standards. When no lipid standard was available, the best possible approximation was used to the correction coefficient obtained with the closest available lipid standard. All sphingolipid measurements in cells were normalized by total lipid phosphorus. All sphingolipid measurements in BALF and plasma were normalized by volume.

*GCS activity assay*

GCS enzyme activity assay was performed according to the methods of David et al (E10) with modifications. Following treatments, culture medium was removed, cells were washed with cold PBS on ice, and collected in lysis buffer (5 mM MOPS, 1 mM EDTA, 250 mM sucrose, 10% glycerol, and freshly added 1 mM PMSF, pH 7.4). Enzymatic reaction was performed in a medium, containing 50 mM HEPES (pH 7.4), 25 mM KCl, 5 mM $MnCl_2$, 2.5 mM UDP-glucose, 10 μM C8-ceramide, and 5 μg of protein (HLMVECs lysate) in a final volume of 0.5 ml at 37°C for 30 minutes. Reaction was stopped by the addition of methanol. Lipids were extracted as described above. Formation of C8-Glc-Cer was determined by the LC-MS/MS by monitoring the transition from the m/z 588.8 to the m/z 264.4

*Endolysosomal pH measurement*

Endolysosomal pH was determined using LysoSensor yellow/blue DND160 (ThermoFisher Scientific) using a previously published method (E11). Briefly, following the treatments, cells were labelled with 5 μM Lysosensor yellow/blue for 5 min at 37 °C. Excess dye was removed by cold PBS. The pH calibration

curve was performed with calibration buffer solutions containing 10 μM monensin, 10 μM nigericin, 25 mM MES, 1.2 mM $MgSO_4$, 115 mM KCL, and 5mM NaCl (pH from 3.0 to 7.0). The emission ratio at 451/520 was measured at Ex 320/360 nm.

*Human lungs*

Human lung tissues from never smokers (*n* = 6) and smokers (*n* = 7) were obtained from deidentified organ donors whose lungs were donated for medical research through the National Disease Research Interchange (Philadelphia, PA) and the International Institute for the Advancement of Medicine (Edison, NJ). These donors had no history of lung disease, acute lung infections, or prolonged mechanical ventilation, and with a $PaO_2/FiO_2$ ratio of >225. Sex, age, or race were not a selection criterion. COPD lungs (*n* =7) were from the Lung Tissue Research Consortium. Lung tissues were stored at -80°C until use. All protocols were approved by the Institutional Review Board at National Jewish Health.

## References

E1. Clauss M, Voswinckel R, Rajashekhar G, Sigua NL, Fehrenbach H, Rush NI, Schweitzer KS, Yildirim AO, Kamocki K, Fisher AJ, Gu Y, Safadi B, Nikam S, Hubbard WC, Tuder RM, Twigg HL, 3rd, Presson RG, Sethi S, Petrache I. Lung endothelial monocyte-activating protein 2 is a mediator of cigarette smoke-induced emphysema in mice. *J Clin Invest* 2011; 121: 2470-2479.

E2. Takeda K, Ning F, Domenico J, Okamoto M, Ashino S, Kim SH, Jeong YY, Shiraishi Y, Terada N, Sutherland ER, Gelfand EW. Activation of p70S6 Kinase-1 in Mesenchymal Stem Cells Is Essential to Lung Tissue Repair. *Stem Cells Transl Med* 2018.

E3. Petrache I, Natarajan V, Zhen L, Medler TR, Richter AT, Cho C, Hubbard WC, Berdyshev EV, Tuder RM. Ceramide upregulation causes pulmonary cell apoptosis and emphysema-like disease in mice. *Nat Med* 2005; 11: 491-498.

E4. Tuder RM, Zhen L, Cho CY, Taraseviciene-Stewart L, Kasahara Y, Salvemini D, Voelkel NF, Flores SC. Oxidative stress and apoptosis

interact and cause emphysema due to vascular endothelial growth factor receptor blockade. *Am J Respir Cell Mol Biol* 2003; 29: 88-97.

E5. Koike K, Beatman EL, Schweitzer KS, Justice MJ, Mikosz AM, Ni K, Clauss MA, Petrache I. Subcutaneous administration of neutralizing antibodies to endothelial monocyte-activating protein II attenuates cigarette smoke-induced lung injury in mice. *Am J Physiol Lung Cell Mol Physiol* 2019; 316: L558-L566.

E6. Iwashita H, Sakurai HT, Nagahora N, Ishiyama M, Shioji K, Sasamoto K, Okuma K, Shimizu S, Ueno Y. Small fluorescent molecules for monitoring autophagic flux. *FEBS Lett* 2018; 592: 559-567.

E7. Bligh EG, Dyer WJ. A rapid method of total lipid extraction and purification. *Can J Biochem Physiol* 1959; 37: 911-917.

E8. Vaskovsky VE, Kostetsky EY, Vasendin IM. A universal reagent for phospholipid analysis. *J Chromatogr* 1975; 114: 129-141.

E9. Berdyshev EV, Gorshkova IA, Garcia JG, Natarajan V, Hubbard WC. Quantitative analysis of sphingoid base-1-phosphates as bisacetylated derivatives by liquid chromatography-tandem mass spectrometry. *Anal Biochem* 2005; 339: 129-136.

E10. Marks DL, Paul P, Kamisaka Y, Pagano RE. Methods for studying glucosylceramide synthase. *Methods Enzymol* 2000; 311: 50-59.

E11. Wheeler S, Haberkant P, Bhardwaj M, Tongue P, Ferraz MJ, Halter D, Sprong H, Schmid R, Aerts J, Sullo N, Sillence DJ. Cytosolic glucosylceramide regulates endolysosomal function in Niemann-Pick type C disease. Neurobiol Dis 2019; 127: 242-252.

**Table E1. Clinical characteristics of study subjects**

| Characteristic | Never smokers (*n* = 6) | Smokers (*n* = 7) | COPD (*n* = 7) |
|---|---|---|---|
| Age, year | 45.2 ± 9.1 | 58.4 ± 7.7 | 66.7 ± 4.3 |
| Male sex, *n* (%) | 4 (66.7) | 3 (42.8) | 3 (42.8) |
| Current smoker, *n* (%) | 0 | 6 (85.7) | 1 (14.2) |
| Smoking history, pack-year | 0 | 37.8 ± 9.9 | 53.8 ± 5.1 |
| $FEV_1$, %of predicted value | — | — | 37.9 ± 5.7 |
| Gold stage, *n* | | | |
| I | — | — | 0 |
| I | — | — | 2 |
| III | — | — | 2 |
| IV | — | — | 3 |

Definition of abbreviations: $FEV_1$ = Forced expiratory volume in one second; GOLD = Global initiative for chronic obstructive lung disease. Post-bronchodilator spirometry was performed on all COPD subjects. The GOLD stages ranges from I, indicating mild disease, to IV, indicating very severe disease.

**Supplemental figure legends**

**Figure E1 Effect of CS and elastase on glucosylceramide (GlcCer) levels in mice.** (**A**) Western blots and densitometric analysis of GCS normalized

to vinculin as loading control in the lungs of C57BL/6 mice were exposed to cigarette smoke (CS) or ambient air control (AC) for 6 months (mean ± SEM; *$P$<0.05 by Mann-Whitney test; $n$ = 5). (**B-C**) GlcCer levels measured by LC-MS/MS in plasma of (**B**) C57BL/6 mice ($n$ = 8) were exposed to CS or AC for 6 months or (**C**) BALB/c mice ($n$ = 8-12) that received intratracheal instillations of elastase (6 U/mouse) or saline control (mean ± SEM; *$P$<0.05 by Mann-Whitney test).

**Figure E2 Effect of GCS inhibition on cell survival and sphingolipid levels in HMVECs.** (**A-B**) Cell viability (**A**) measured by CCK-8 kit and LDH release (**B**) in HLMVECs treated with vehicle or Genz (1 or 2 or 5 or 10 μM; 6 hours) (mean ± SEM; **$P$<0.01 and ***$P$ < 0.001, one-way ANOVA with Tukey's multiple comparisons test; $n$ = 3). (**C-F**) Levels of Ceramide (**C**), sphingosine-1-phosphate (S1P) (**D**), sphingomyelin (**E**), and sphingosine (**F**) measured by LC-MS/MS in HLMVECs treated with vehicle or Genz (2 μM; 6 hours; $n$ = 5). Absolute levels of ceramide shown here are representative of five independent experiments. (**G-H**) Representative western blots and densitometry of Bax, Bcl-2 (**G**) and IRE1α (**H**) in HLMVECs treated with vehicle or Genz (2

μM; 6 hours) (mean ± SEM; *$P$<0.05 by Mann-Whitney test; $n$ = 3-4). Western blots shown are representative of at least three independent experiments.

**Figure E3 Effect of GCS inhibition on ceramide levels and mTOR signaling in HMVECs.** (**A**) Schematic of mTOR signaling pathway. (**B-F**) GCS mRNA expression and ceramide levels in HLMVECs transfected with 5 nM of control siRNA (siNT) or siRNA against GCS (siGCS) for 72 hours ($n$ = 3). (**B**) GCS mRNA expression. (**C**) Ceramide levels (fold change vs. siNT) from three independent experiments (#1, #2, and #3) ($n$ = 3). (**D**) Absolute ceramide levels from experiment #1 ($n$ = 1). (**E**) Absolute ceramide levels from experiment #2 ($n$ = 1). (**F**) Absolute ceramide levels from experiment #3 ($n$ = 1). (**G-H**) Cell viability (**G**) determined by trypan blue exclusion assay and LDH release (**H**) in HLMVECs transfected with 5 nM of control siNT or siGCS for 96 hours (n = *3*). (**I-J**) Representative western blots and densitometric analysis of phospho (p-) and total AKT (**I**) and p- and total AMPKα (**J**) in HLMVECs treated with vehicle or Genz (2 μM) for 30 minutes. All graphs shows as mean ± SEM; *$P$ < 0.05 by Mann-Whitney test.

**Figure E4 Effect of GCS inhibition on autophagy in HLMVECs.** (**A-B**) Densitometric analysis of LC3B-II (**A**) and SQSTM1 (**B**) in HLMVECs treated with vehicle or Genz (2 μM) for 6 hours, while treated with either vehicle (DMSO), chloroquine (CQ, 20 μM), or bafilomycin A1 (BafA1, 5 nM) for 6 hours (*n* = 3).

(**C**) Representative western blots and densitometric analysis of LC3B-II and SQSTM1 in HLMVECs transfected with 5 nM of siNT or siGCS for 72 hours and treated with either vehicle or bafilomycin A1 (BafA1, 5 nM) for 6 hours (*n* = 4). Vinculin was used as loading control. Western blots shown here are representative of three independent experiments. All graphs shows as mean ± SEM; **P* < 0.05 and ***P* < 0.01 by one-way ANOVA with Tukey's multiple comparisons test.

**Figure E5 Effect of CSE on apoptosis, mTOR signaling, and autophagy in HLMVECs.** (**A-B**) Cell viability (**A**) determined by trypan blue exclusion assay and LDH release (**B**) in HLMVECs exposed to AC or 3% CS extract (CSE) for 6 hours (*n* = 3). (**C-E**) Representative western blots and densitometric analysis of Bax, Bcl-2 (**C**), cleaved caspase-3 (**D**), and phospho

(p-) and total S6 ribosomal protein (S6) (**E**) in HLMVECs exposed to AC or 3% CSE for 6 hours (*n* = 3-5). **(F**) Representative western blots and densitometric analysis of LC3B and SQSTM1 in HLMVECs treated with AC or 3% CSE for 6 hours, while treated with vehicle (DMSO) or BafA1 (5 nM) for 6 hours. β-actin was used as loading control (*n* = 3). (**G**) Representative immunofluorescence images of HLMVECs treated with either AC, 3% CSE, BafA1 (5 nM), or 3% CSE plus BafA1 (5 nM) for 6 hours. Following treatments, cells were incubated with DAPGreen (50 nM) and LysoTracker deep red (25 nM) for 30 minutes. Scale bar: 20 μm. Western blots and immunofluorescence images are representative of at least three independent experiments. All graphs shows as mean ± SEM; **P* < 0.05 and ***P* < 0.01 by one-way ANOVA with Tukey's multiple comparisons test or Mann-Whitney test.

**Figure E6 Effect of GlcCer treatment on apoptosis and impaired autophagic flux in GCS-inhibition or CSE-exposed HLMVECs.**

(**A**) Absolute endogenous GlcCer levels measured by LC-MS/MS in HLMVECs treated with vehicle (ethanol) or admantyl GlcCer (1 μM; 30 hours). GlcCer levels shown here are representative of three independent experiments. (**B)**

Representative western blots of cleaved PARP1 in HLMVECs incubated with either vehicle or admantyl GlcCer (1 μM; 24 hours) and exposed to vehicle or Genz (2 μM; 6 hours). (**C-D**) Representative western blots and densitometric analysis of cleaved PARP1 (**C**), LC3B and SQSTM1 (**D**) in HLMVECs incubated with either vehicle or admantyl GlcCer (1 μM) for 24 hours and treated with AC or CSE (3%; 6 hours). β-actin was used as loading control (*n* = 3). (**E**) Representative immunofluorescence images of HLMVECs incubated with vehicle or admantyl GlcCer (1 μM) for 24 hours and treated with either AC or 3%CSE for 6 hours. Following treatments, cells were incubated with DAPGreen (50 nM) and LysoTracker deep red (25 nM) for 30 minutes. Arrowhead indicates colocalization between autophagosome and lysosome. Scale bar: 20 μm. Western blots and immunofluorescence images are representative of at least three independent experiments. All graphs shows as mean ± SEM; **P*<0.05 and ***P* < 0.01 by one-way ANOVA with Tukey's multiple comparisons test.

**Figure E7 Effect of GCS overexpression on sphingolipids in HLMVECs.** (**A-E**) Levels of GlcCer (**A**), ceramide (**B**), S1P (**C**), sphingomyelin (**D**), and sphingosine (**E**) measured by LC-MS/MS in HLMVECs transfected with

1 μg of GCS-tGFP or Ctr-tGFP for 24 hours and treated with AC or CSE (3%; 6 hours; *n* = 3-4). All graphs shows as mean ± SEM; **P*<0.05 and ***P* < 0.01 by one-way ANOVA with Tukey's multiple comparisons test.

**Figure E8 Decreased GCS levels in COPD lungs.** (**A**) Western blots and densitometric analysis of GCS in the lungs from never smokers (healthy) vs. smokers with COPD. (**B**) Western blots and densitometric analysis of GCS in the lungs from smokers without COPD vs. smokers with COPD. GAPDH was used as loading control. All graphs shows as mean ± SEM; ***P*<0.01 by Mann-Whitney test; n = 6-7.

# Supplemental Figure E1

A

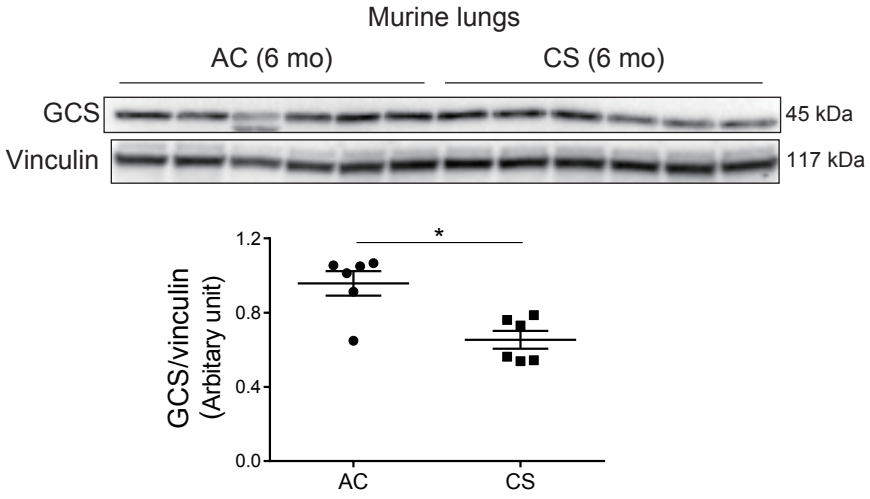


B

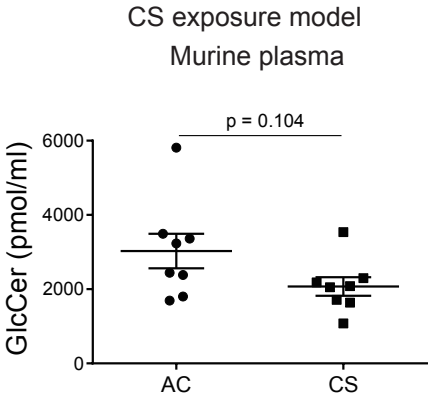


C

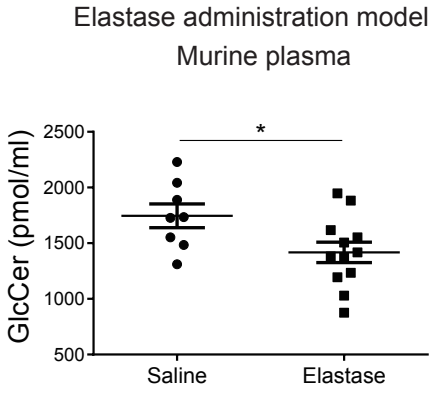

# Supplemental Figure E2

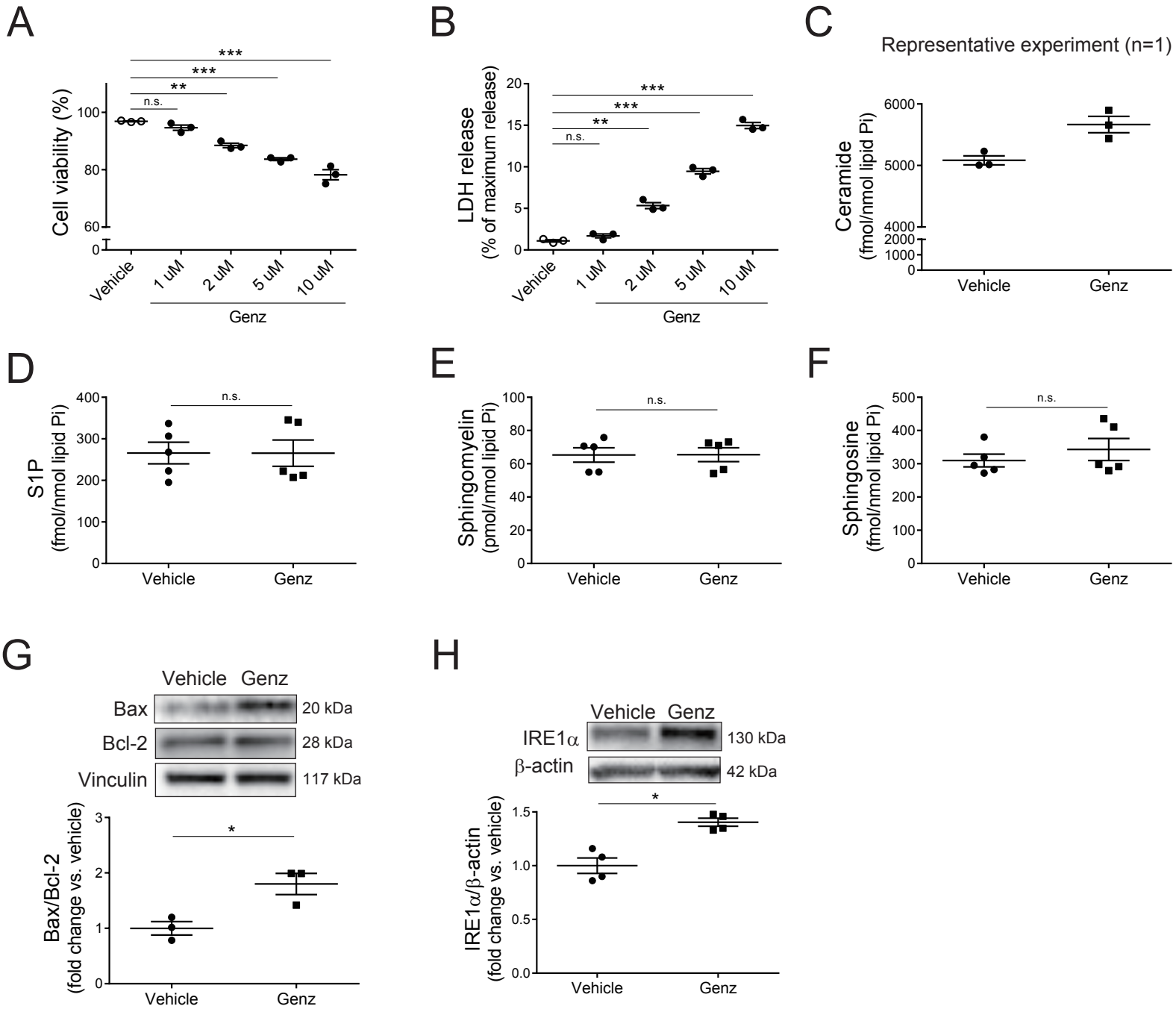

# Supplemental Figure E3

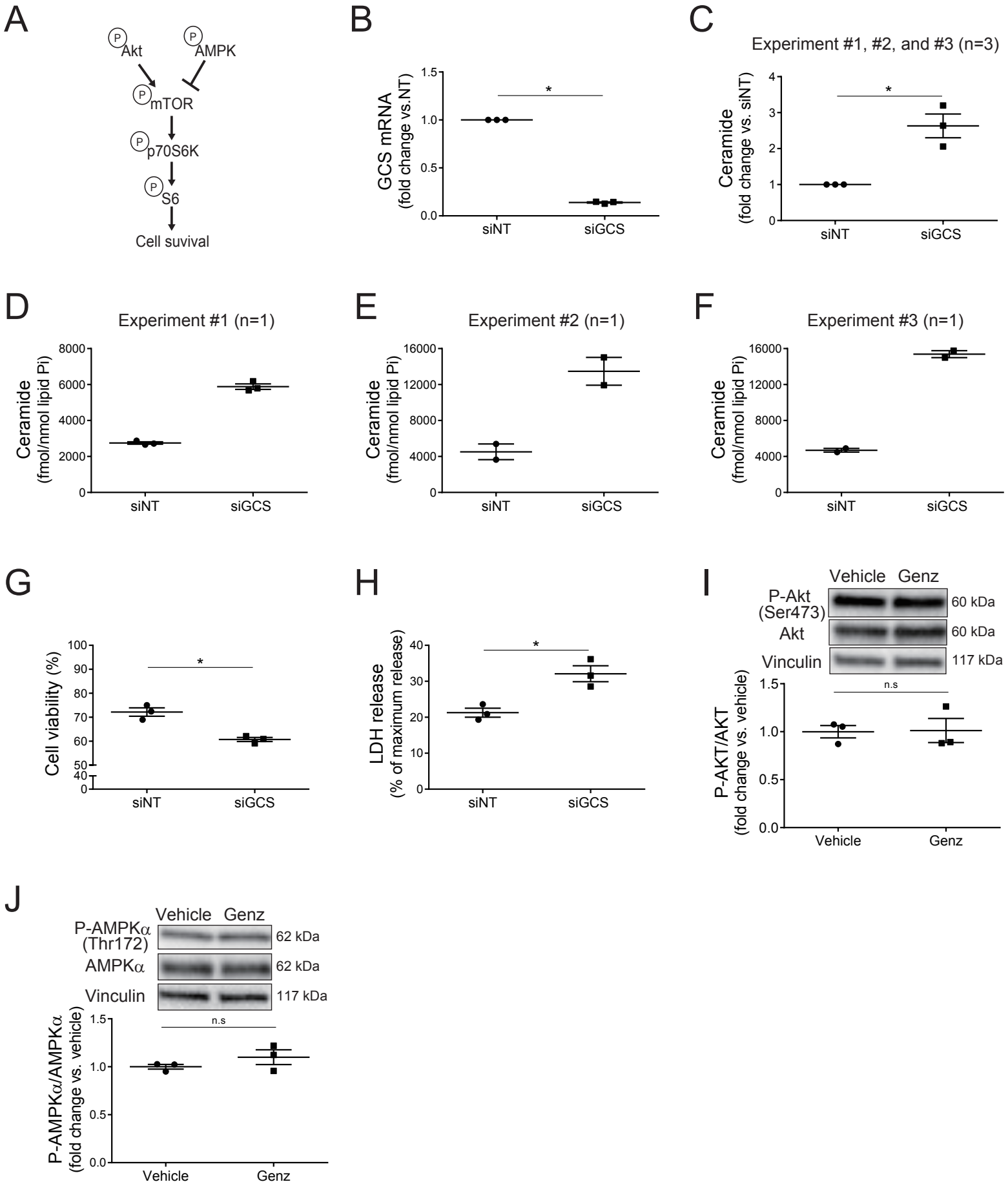

# Supplemental Figure E4

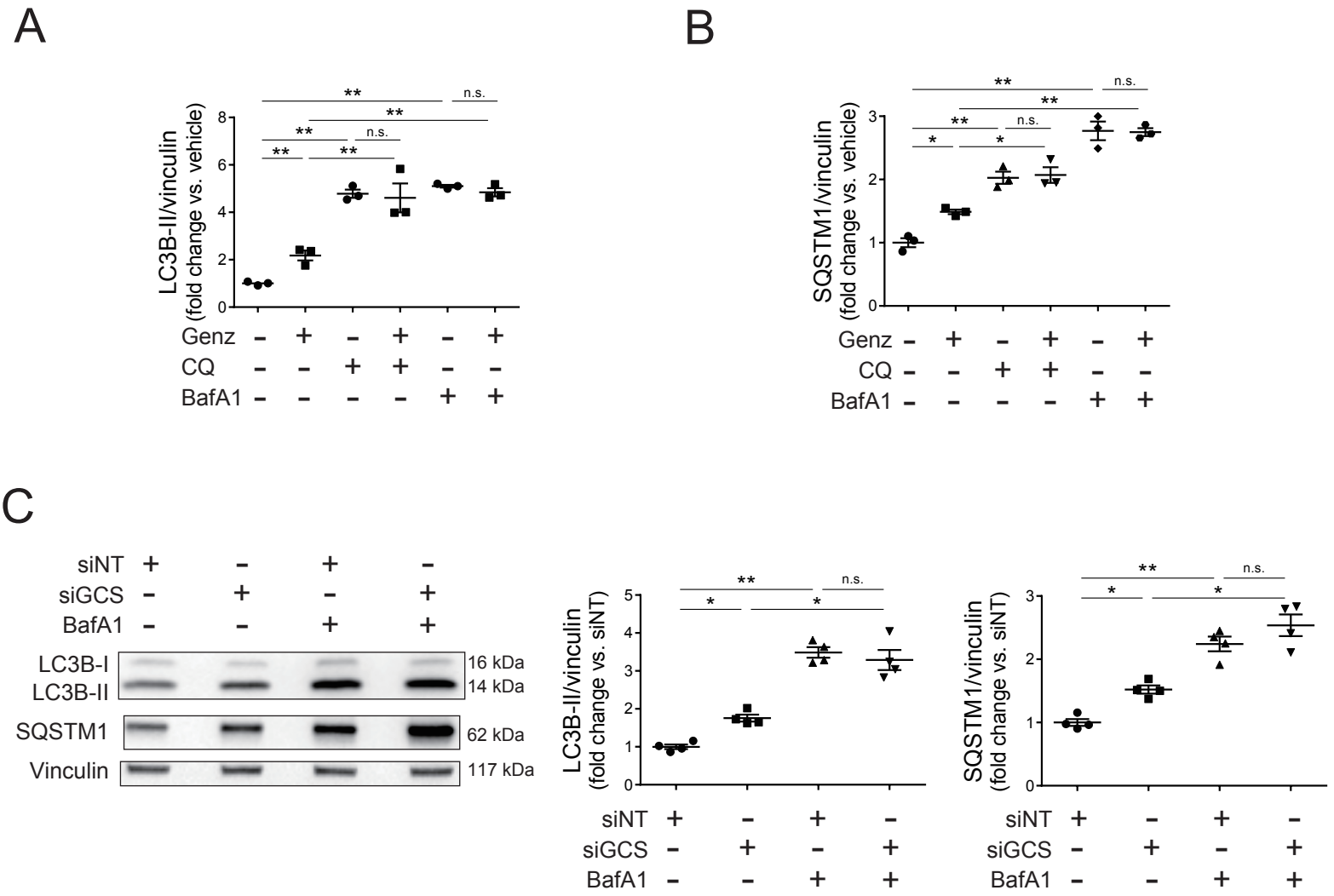

# Supplemental Figure E5

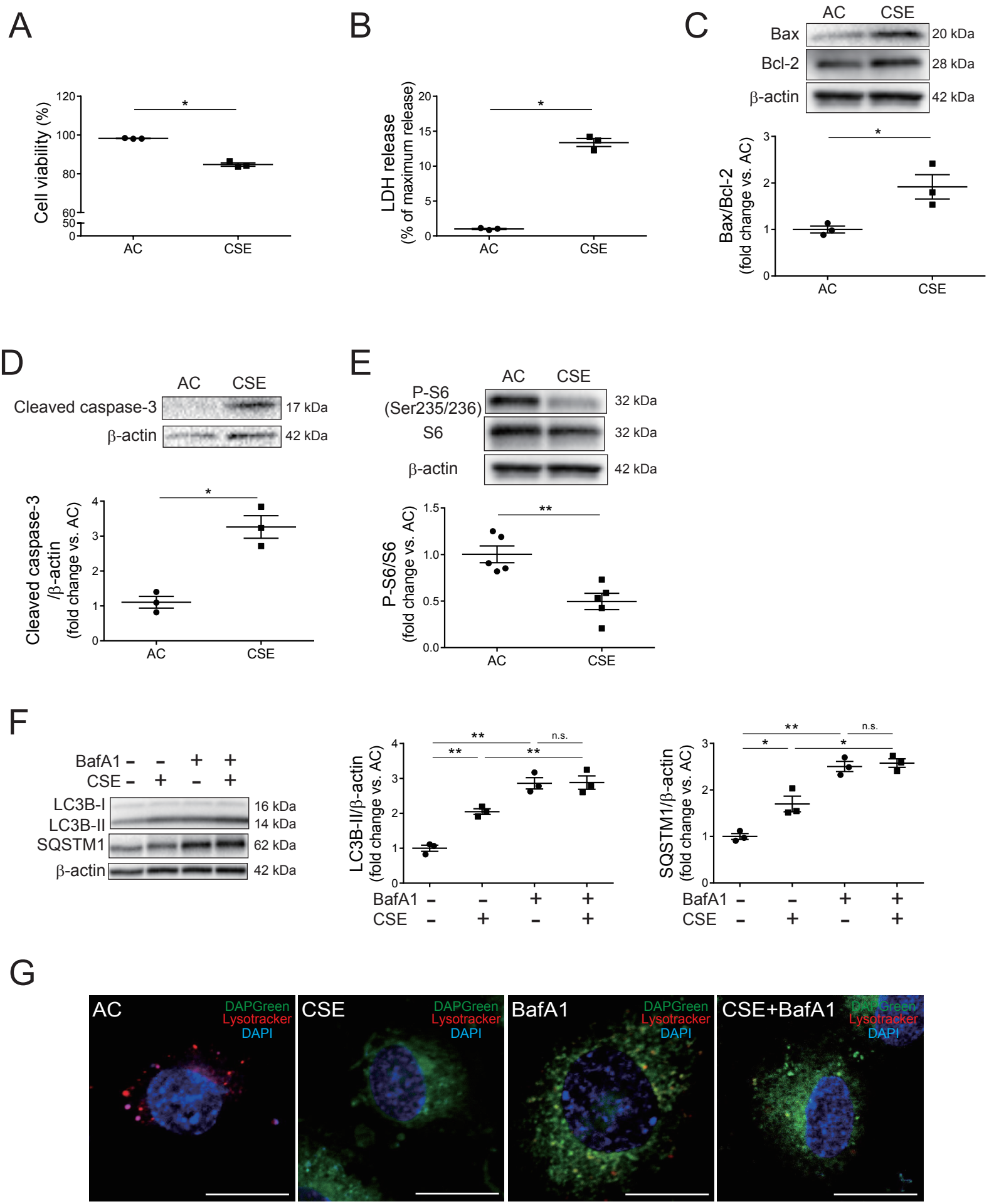

# Supplemental Figure E6

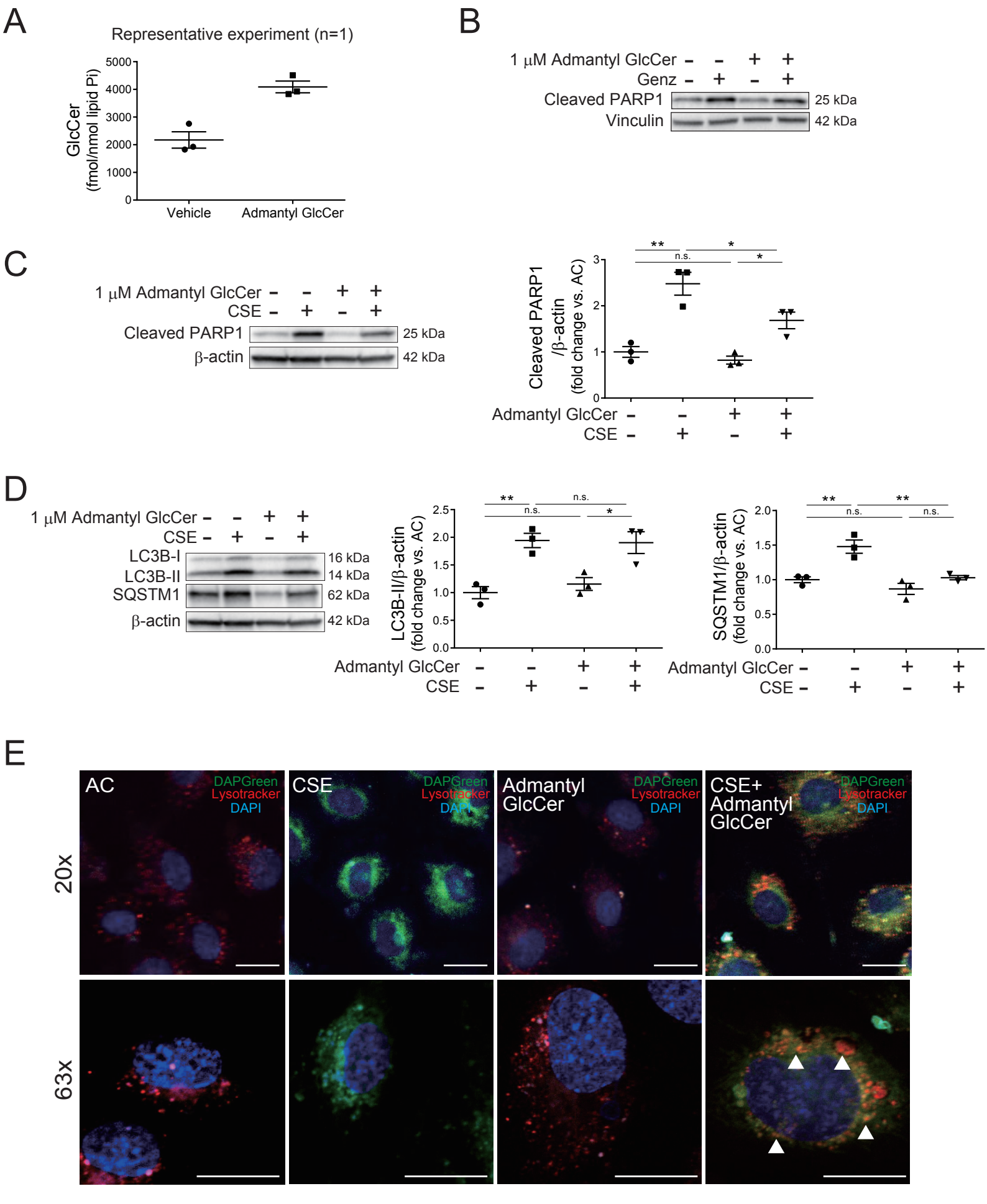

# Supplemental Figure E7

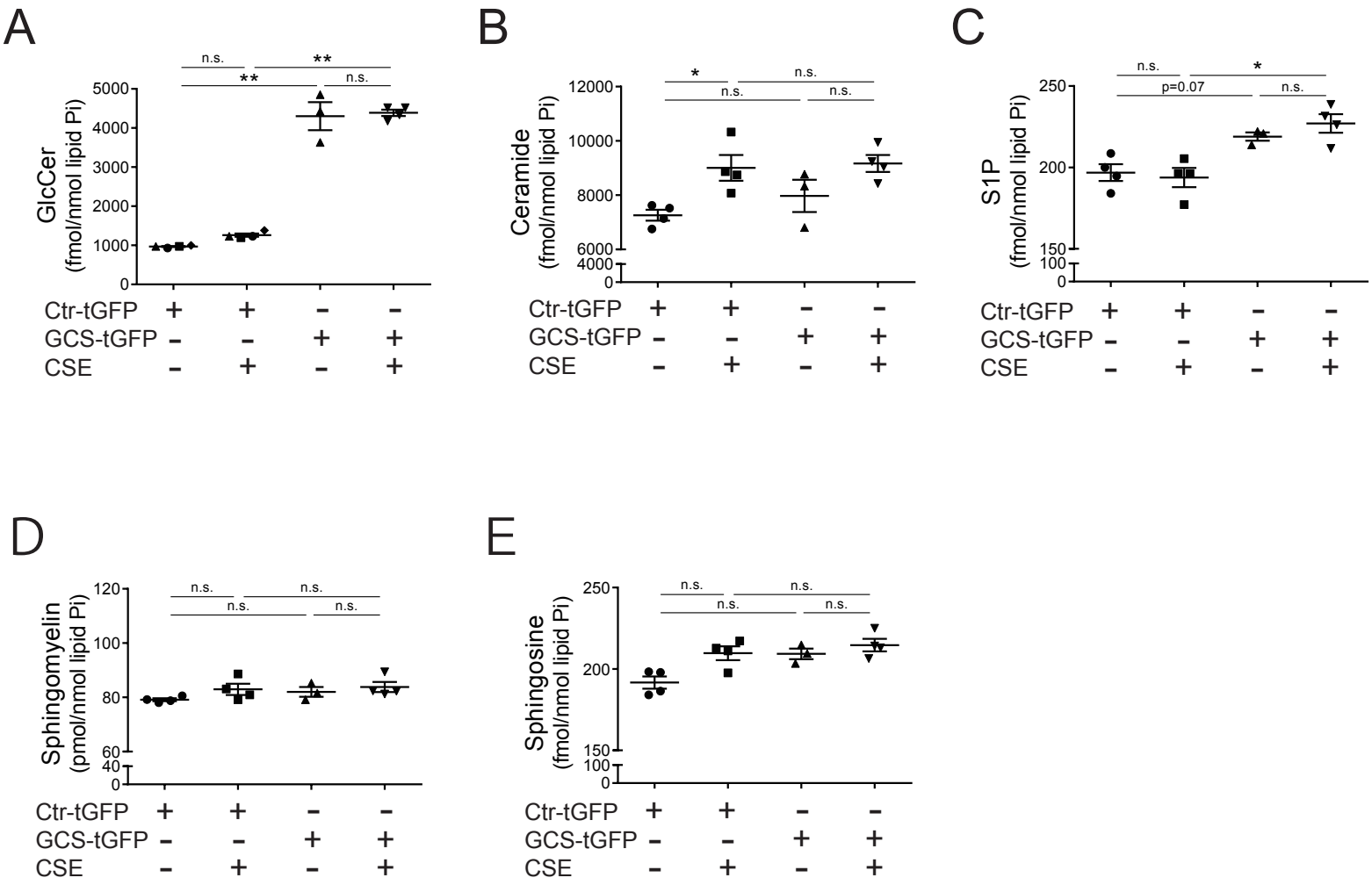

# Supplemental Figure E8

A

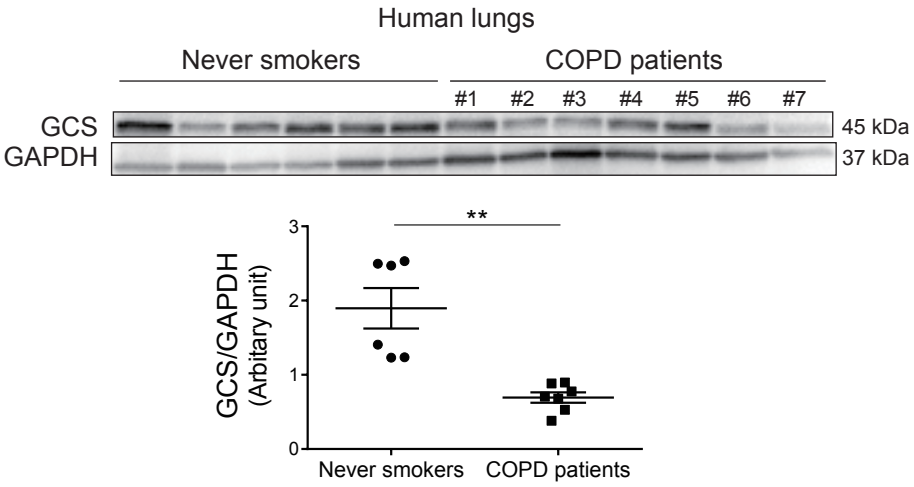


B